CONF-790816--10

BNL-NUREG-25498

A SINGLE-PHASE SODIUM PUMP MODEL FOR LMFBR THERMAL-HYDRAULIC ANALYSIS†

Imtiaz K. Madni, Erik G. Cazzoli, and Ashok K. Agrawal

Department of Nuclear Energy
Brookhaven National Laboratory
Upton, New York 11973 USA

ABSTRACT

A single-phase, homologous pump model has been developed for simulation of safety-related transients in LMFBR systems. Pump characteristics are modeled by homologous head and torque relations encompassing all regimes of operation. These relations were derived from independent model test results with a centrifugal pump of specific speed equal to 35 (SI units) or 1800 (gpm units), and are used to analyze the steady-state and transient behavior of sodium pumps in a number of LMFBR plants. Characteristic coefficients for the polynomials in all operational regimes are provided in a tabular form. The speed and flow dependence of head is included through solutions of the impeller and coolant dynamic equations. Results show the model to yield excellent agreement with experimental data in sodium for the FFTF prototype pump, and with vendor calculations for the CRBR pump. A sample pipe rupture calculation is also performed to demonstrate the necessity for modeling the complete pump characteristics.

†This work was performed under the auspices of the U.S. Nuclear Regulatory Commission.

A SINGLE-PHASE SODIUM PUMP MODEL FOR LMFBR THERMAL-HYDRAULIC ANALYSIS

Imtiaz K. Madni, Erik G. Cazzoli, and Ashok K. Agrawal

1. INTRODUCTION

A major question in LMFBR safety analysis is whether sufficient cooling capability is provided to keep fuel cladding temperatures within a specified limit for a variety of transients. The behavior of the centrifugal pumps which circulate the reactor coolant can be very important, at least for certain transients. An adequate model for these sodium pumps must, therefore, be provided in any thermo-hydraulic plant simulation code.

The degree of modeling sophistication for the pumps depends on the nature of transients that may be investigated. For example, for a loss-of-piping-integrity accident in the primary heat transport system, the conditions imposed on the pump are determined by the type of accident postulated (location and size of rupture), pump location (whether in broken or intact loop), and the thermal-hydraulic response of the rest of the system. The flow through the pump may completely reverse direction, as can the impeller rotation, causing the pump to go through several regimes of operation.

Existing LMFBR plant codes, e.g., IANUS,[1] which was designed to simulate the overall performance of the Fast Flux Test Facility (FFTF) and DEMO,[2] designed for the Clinch River Breeder Reactor Plant (CRBRP), model the sodium pump performance for their respective plants, based on vendor-supplied data for the unit in question. Also, taking credit for the presence of anti-reverse rotation devices, these characteristic data provide for operation only in regimes where speeds are greater than or equal to 0 rpm.

The aim of this paper is to present a generalized pump model that was developed for the Super System Code (SSC).[3] This component model is designed to be applicable to the sodium pumps in a whole class of LMFBR plants, including FFTF and CRBR (loop-type, USA), SNR (loop-type, Germany), PHENIX (pool-type, France), etc. Further, to allow for the possibility of absence or failure of anti-reverse rotation devices, the model represents pump performance encompassing all regimes of operation, including those with reverse speed and/or flow. The complete characteristics are represented as homologous polynomial relations and were obtained from independent model tests[4,5] with a centrifugal pump of specific speed equal to 35 (SI units) or 1800 (gpm units).

In the following sections, model development and assumptions will be described, together with a brief discussion of system thermal-hydraulics with which the model interfaces to account for the mutual interactions between pump and system. Characteristic coefficients for all regimes of pump operation are provided in a tabular form. Some comparisons of the present model will be shown with available experimental data from FFTF prototype pump testing in sodium at the Liquid Metal Engineering Center (LMEC), and with vendor calculations. Representative results of a sample pipe rupture calculation obtained with the model will also be presented and discussed.

2. ANALYSIS

All currently designed main sodium pumps for LMFBRs are vertically mounted, centrifugal units, with the impeller at the bottom of the shaft. The main motor, residing at the top of the shaft, is generally variable speed (an exception is PFR, where a fixed speed motor is hydraulically coupled to the shaft with variable speed ratios). The primary purpose of the analytical pump model is to calculate the pressure rise across the pump for use in coolant dynamic analysis of the heat transport system. The speed and flow dependence of the pressure rise or head, is included through solutions of the impeller and coolant dynamic equations. This yields a variable pump head, dependent on transient conditions.

The impeller is modeled in terms of homologous head and torque relations which describe pump characteristics, and angular momentum balance to determine transient impeller speed. Where a separate free surface of sodium with its associated cover gas space exists in the pump, a free-surface pump tank is modeled just upstream of the impeller.

The analysis is based on the following simplifying assumptions:

i) The impeller is a single control volume.

ii) Flow rate into the impeller is equal to flow rate out (i.e., no mass accumulation around the impeller).

iii) Pump characteristics, based on steady-state data, are applicable during transient operation. This assumption implies that the instantaneous performance of the turbomachine at any time during a transient is identical with the steady-state performance for the same operating conditions. This type of assumption is commonly used in other thermal-hydraulic work as well, where, for example, heat-transfer correlations and friction factors, obtained

during steady-state conditions, are applied to transient analysis.

iv) Scale effects are considered negligible, and

v) Single-phase model (no cavitation effects).

2.A Homologous Characteristics

Figure 1 shows, in sequence, the different operating modes a pump may experience during a transient. During most operational transients and even loss-of-electric-power incidents involving simultaneous coastdown of all pumps, the impeller may stay within the normal operating regime. However, a severe asymmetric transient such as caused by a double-ended pipe rupture near the reactor vessel inlet could send the impeller through all four regimes (assuming absence or failure of anti-reverse devices).

Pump manufacturers generally supply performance data of their units for normal operation only. Due to practical limitations additional data is available from scaled-down models, not necessarily with liquid metal, and from selected combinations of operating conditions within the capabilities of the test facility. To obtain the complete characteristics (performance curves encompassing all four operational regimes shown in Figure 1) we resort to homologous theory[5], whereby if the pump parameters head (H), torque (τ_{hyd}), discharge ($Q=\frac{W}{\rho}$) and speed (Ω), are divided by their respective rated values, the non-dimensional (homologous) characteristics (h, β, ν, α) obtained are independent of the liquid pumped and the slope of the characteristic curves depends only on N_s, the rated specific speed.[4,6] This assumes negligible viscosity effects. In general, the influence of viscosity and other scale effects on pump head and torque is small for single-phase flow.[7]

Based on this theory, the performance data from Streeter and Wylie[5] and Donsky[4] for a single-stage centrifugal pump with N_s=35 (SI units)

or 1800 (gpm units) were fitted with polynomials of the following form:

$$\frac{h}{\alpha^2} \text{ or } \frac{\beta}{\alpha^2} = \sum_{i=0}^{n} c_i \left(\frac{\nu}{\alpha}\right)^i \qquad 0 \leq \left|\frac{\nu}{\alpha}\right| \leq 1 \qquad (1)$$

$$\frac{h}{\nu^2} \text{ or } \frac{\beta}{\nu^2} = \sum_{i=0}^{n} c_i \left(\frac{\alpha}{\nu}\right)^i \qquad 0 \leq \left|\frac{\alpha}{\nu}\right| < 1 \qquad (2)$$

A least square, random search and gradient search procedure[8] was applied to determine c_i's for $2 \leq n \leq 7$. The best accuracy and smoothness of fit was obtained with $n = 5$ for each region except reverse pump where the limited number of data points caused smoother fits with lower order polynomials. Seven head and seven torque curves have thus been defined through all operational regions with an accuracy of 1% or better. The corresponding c_i's are provided in Table 1. Appendix A describes the logic to switch from one operating region to another during the transient computations.

The value of specific speed of 35 (1800)* lies in the range of specific speeds for LMFBR pumps (e.g., for FFTF, $N_s \simeq 27.2$ (1400); PHENIX, $N_s \simeq 36.9$ (1900); SNR, $N_s \simeq 40.8$ (2100); CRBR, $N_s \simeq 42.8$ (2200)) and homologous theory would then suggest that the data of Table 1 can be used directly to characterize the sodium pumps in any of these plants. In comparison, specific speed for LWR pumps is of the order of 100 (5000). In the next section, some validation of this will be provided through comparisons with experimental measurements, and with other models based on vendor-supplied pump data.

*The numbers indicate rated specific speed in SI units followed by gpm units in parenthesis.

2.B Steady-State Model

Pump operating speed (Ω) during steady-state is determined by matching required pump head with total hydraulic resistance in the circuit. For example, for the primary pumps, the required pressure rise is obtained from

$$\Delta P_p = \sum_j \Delta P_j + \Delta P_{CV} + \Delta P_{RV} \tag{3}$$

where ΔP_j's are the pressure drops in the pipes and/or components e.g., IHX. ΔP_{RV} and ΔP_{CV} are, respectively, the pressure drops in the reactor vessel and check valve.

Pump head is related to ΔP_p by:

$$H = \Delta P_p/(\rho_{in} g) \tag{4}$$

Knowing H and the flow rate, Equation (1) can be rearranged to give a polynomial in α, which is solved for α (hence $\Omega = \alpha\Omega_R$) by a Newton's method specially adapted for polynomials.

2.C Dynamic Model

Once the characteristics are available in the form of Equations (1) and (2), the transient head and torque can be determined, knowing rated values, operating speed and flow rates. The transient pump speed equation is obtained from angular momentum balance at the shaft and rotating assembly as

$$I \frac{d\Omega}{dt} = \tau_m - \tau_{hyd} - \tau_{fr} \tag{5}$$

Here, I is the moment of inertia (designer-specified), and τ_m the applied motor torque (=0 during coastdown); τ_{hyd} is the load torque due to fluid at the impeller, obtained from homologous torque curves (Equation (2)), and

τ_{fr} is the frictional torque due to bearing losses, fluid friction, etc. This is represented in the model as polynomial equations in α (See Appendix B).

Where there is a separate free-surface pump tank modeled upstream of the impeller, mass balance yields the equation describing coolant level Z_R in the pump tank as:

$$A_R \frac{d}{dt} (\rho Z_R) = W_{in} - W_{out} \tag{6}$$

Coolant density (ρ) variations are included. Where no separate pump tank is modeled (e.g., primary pumps in pool-type LMFBRs), $W_{in} = W_{out}$.

To analyze the pump behavior, it has to be coupled to the rest of the system. Figure 2 illustrates an example configuration of the primary heat transport system of a loop-type LMFBR plant, for two-loop simulation of a multi-loop system. One of the loops has a pipe-break near the reactor vessel and all intact loops are lumped together as the other loop. The pumps are shown located in the hot leg. This corresponds to the CRBR (or FFTF) primary loop design. There is one pump for each primary heat transport loop. For a pump coastdown transient, one loop simulation with all three loops being lumped together is sufficient. The configuration would look much like Figure 2 without the broken loop. In our discussions here, we focus attention on the primary system due to its more direct impact on core flow. Similar analysis is performed for the intermediate circuits.

System flow rates are described by equations of the form

$$\frac{dW}{dt} \sum \frac{L}{A} = P_{in} - P_{out} - \sum \Delta P_{f,g} \tag{7}$$

for each uniform mass flow rate section.[3] Here $\sum \frac{L}{A}$ is the fluid

inertia; P_{in}, P_{out} are the endpoint pressures; and $\sum \Delta P_{f,g}$ is the sum of frictional, gravitational and all other losses in the section. The gravitational loss (gain) is dependent on elevations and sodium density distributions. The coolant density at any location is a function of temperature, obtained from system thermal calculations. At pump location, the end pressures of adjacent sections are related by ΔP_p ($=\rho_{in} gH$), obtained from Equation (1).

The arguments presented above can be carried over essentially intact to the pool-type primary system, where the pumps and IHX's are immersed in a pool of sodium.

3. RESULTS

3.A Comparison with Experimental Data and Other Models

Comparisons were made with some high temperature in-sodium test results of the FFTF prototype primary pump obtained at LMEC.[9] The FFTF prototype pump is designed to deliver 0.9148 m^3/s (14,500 gpm) of sodium at 153.3 m (503 ft) total head and 1110 rpm, corresponding to design temperature of 838.7 K (1050°F). Figures 3 and 4 show comparisons of pump head as computed by the present model and the IANUS model with the measured data for various speeds and flows. The IANUS model is based on vendor-supplied performance data for the FFTF pump. Three different sets of data points in Figure 3 correspond to pump performance at the minimum operational, design, and maximum loop hydraulic resistances. Agreement between the two models and the test data is very good. Figure 4 shows the predictions to fall within ± 5% of the measured values.

Yang and Madni[10] compared locked rotor pressure drop characteristics for the FFTF pump as computed by IANUS and the present model with experimental data, and found the present model to give better agreement with the measurements than IANUS. Since the data of Table 1 was derived independently based on performance characteristics of a model centrifugal pump with N_s=35 (SI units), these comparisons indicate that the present model can also be used to represent a prototype pump (FFTF) with N_s=27.2.

Comparisons were also made with vendor-supplied results for the CRBR primary sodium pumps (N_s=42.8). In the CRBR PSAR,[11] the expression for pump locked rotor impedence to forward flow is presented as

$$H = - 250\, v^2 \quad \text{(in ft of Na)}$$

With a rated pump head of 458 ft, this reduces to

$$h = 0.546\ v^2 \qquad (8)$$

From Table 1, for $\alpha = 0$ in the HVN curve we get

$$h = -\ 0.556\ v^2 \qquad (9)$$

Equations (9) and (10) are in close agreement, with the present model yielding a 2% higher value of pressure drop than that of the vendor.

To compare the characteristics in the present model with those in DEMO (based on vendor-supplied data for CRBR pumps, in normal operation region only), a pump coastdown-to-natural-circulation analysis was performed using the SSC-L code. Figure 5 shows predicted speed and flow decay for a 120 second transient. The calculated results from the SSC-L code using the two models in turn agree so closely that the differences are not detectable in Figure 5. These comparisons for the CRBR primary pump indicate that the present model is also adequate to analyze pumps with $N_s \simeq 42.8$.

3.B Sample Pipe Rupture Calculations

A double-ended rupture with break area (A_b) equal to the pipe cross-sectional area (A_p) was postulated to occur in the primary cold-leg piping near the reactor vessel inlet, with check valve failure. Note that A_b is defined as the surface area of the cylinder formed between the broken ends, i.e.,

$$A_b = \pi DL$$

With this definition, a double-ended rupture with $A_b = A_p$ represents a separation distance (L) between the two broken ends equal to $\frac{D}{4}$.

Again, calculations were performed using the SSC-L code, with the present model. Computed results are shown collapsed into the homologous

head curves of Figure 6. During the first half-second following break, the pump discharge increases beyond its steady-state value due to the suddenly decreased flow resistance, and with speed decaying, the operating points progress downward along the HVN curve. Looking at the pump behavior in the broken loop, at t = 4 seconds, the downward trend along HVN is reversed due to flow loss at the break, and the pump operation moves up along HVN until, at t = 20 seconds, $\alpha = \nu$. For t > 20 sec, $\frac{\alpha}{\nu} > 1$, and the transient moves into HAN curve. At this point, the guard vessel fills completely, stopping further break flow, and the intact loops attain communication with the rest of the broken loop, causing rapid flow decay leading to flow reversal through the affected pump. The pump operation therefore enters the HAD curve. Following flow reversal, pump speed starts decaying more rapidly. The combined effect of decreasing positive pump speed and increasing negative flow rate causes $\left|\frac{\nu}{\alpha}\right|$ to exceed 1, and the transient moves into HVD. At t = 50 sec, pump speed also reverses, and pump operation enters the HVT curve. Once in the turbine regime, the speed continues to increase in the negative direction until, at t = 76 sec, $\left|\frac{\nu}{\alpha}\right|$ is again less than 1, and the pump enters the HAT curve.

The intact loop pump travels more slowly through its characteristics so that at 52 sec, it is still in normal operation zone. Once flow reverses in the intact loop, however, it travels more rapidly along its characteristics. In fact, it even enters the reverse pump region when, at t = 115 sec, the flow in intact loop recovers.

This transient was picked as an example. Other less severe asymmetric events such as a pipe rupture in the hot-leg piping between the reactor outlet and pump, or a single pump coastdown without reactor scram, would also send the affected pump through abnormal operational regimes, requiring adequate representation of the characteristics for those regimes.

4. DISCUSSION

A single-phase pump model for system transient analysis of LMFBRs has been presented where homologous characteristic curves, derived from a model centrifugal pump with $N_s = 35$, are used to predict the steady-state and transient behavior of sodium pump impellers in LMFBRs. From the results presented, the following inferences are derived:

1) The present homologous model gave predictions that agreed closely with measured data for FFTF pumps ($N_s \simeq 27.2$), performing at least as well as the IANUS model based on vendor data. It also produced excellent agreement with vendor calculations for the CRBR pump ($N_s \simeq 42.8$). These results provide strong credibility to the model for analysis of other full-scale LMFBR sodium pumps such as those in PHENIX ($N_s \simeq 36.9$), SNR ($N_s \simeq 40.8$), etc.
2) From the sample pipe rupture calculations we can infer that representation of pump characteristics for all regimes of operation including those with reverse flow and/or speed, forms an essential part of the model.

For future work, it will be necessary to study the effects of cavitation on pump performance during severe transients such as caused by a double-ended pipe rupture in the primary system with delayed pump trip. A model for cover gas flow into and out of the pump tank may be required to accurately simulate transients from a break in the vicinity of the pump. Experimental data is needed on frictional losses in liquid metal pumps as a function of flow and speed, both in the forward and reverse direction. Finally, even though there is evidence[12,13] to support the use of quasi-steady pump performance data to analyze transient pump performance, it may be worthwhile to experimentally investigate the limits of applicability of this procedure.

APPENDIX A

For the reader's convenience, a flow diagram is presented in Figure A.1, where, with known flow and speed, the operational regime (normal, energy dissipation, turbine, reverse pump) and curve number (I = 1,2,...,7) are identified, and then corresponding head and load torque are evaluated during transient computations. This logic will facilitate direct application of the coefficients presented in Table 1.

APPENDIX B

Pump Friction

The torque due to frictional losses in the pump (see Equation (5)) is represented in the model as polynomial equations of the form

$$\tau_{fr} = \tau_R \left(c_0 + c_1\alpha + c_2\alpha|\alpha|\right) \qquad (B.1)$$

τ_{fr} is highly design dependent, hence not amenable to generalized modeling. However, Equation (B.1) with the appropriate selections of c_0, c_1, c_2 is felt to be adequate to represent most LMFBR pumps.

Representative coefficients used for transient simulations of the present paper are

$$\begin{aligned} &c_0 = 0.012, \quad c_1 = 0.023, \quad c_2 = 0.0 && \text{for } \alpha > 0.0117 \\ &c_0 = 0.117, \quad c_1 = -8.97, \quad c_2 = 0.0 && \text{for } \alpha \leq 0.0117 \\ &c_0 = 0.005, \quad c_1 = 14.77, \quad c_2 = 0.0 && \text{for } 0 \leq \alpha \leq 0.005 \end{aligned} \qquad (B.2)$$

c_0, c_1 for the first two regions were obtained from the equations in DEMO. (These have in large part been derived from pump vendor data for CRBR pumps at higher speeds[14]). However, a two-region model gives unrealistically high values of τ_{fr} for very low speeds (approaching locked rotor). So, a third region has been defined based on start-up torque tests on the FFTF prototype pump.[9] This gives the correct limit for $\alpha = 0$, and results in a realistically small $\frac{d\Omega}{dt}$ at very low speeds and flows, thereby removing any stiffness that would be caused in the dynamic equations otherwise.

For $\alpha < 0$, since flow is fairly large, τ_{fr} has negligible influence on the system response.

NOMENCLATURE

A	Flow or cross-sectional area,	m^2
A_p	Pipe cross-sectional area,	m^2
D	Pipe inner diameter,	m
H	Pump head,	m
L	Normalized pump head (H/H_R)	
I	Moment of inertia,	$kg\text{-}m^2$
L	Length of pipe section,	m
N	Pump speed,	rpm
N_s	Rated pump specific speed, $N_R\sqrt{Q_R}/H^{3/4}$	
P	Pressure,	N/m^2
Q	Volumetric discharge,	m^3/s
W	Mass flow rate,	kg/s
α	Normalized pump speed (Ω/Ω_R)	
β	Normalized hydraulic torque (τ_{hyd}/τ_R)	
ΔP	Pressure loss (or drop),	N/m^2
ν	Normalized pump discharge (Q/Q_R)	
ρ	Coolant density,	kg/m^3
τ_{hyd}	Hydraulic (load) torque,	N-m
τ_R	Rated hydraulic torque,	N-m
Ω	Pump speed,	rad/s
Subscript		
R	Rated value	

REFERENCES

1. S. L. Additon, et al., "Simulation of the Overall FFTF Plant Performance," Hanford Engineering Development Laboratory, HEDL-TC-556 (December 1975).
2. "LMFBR Demonstration Plant Simulation Model, DEMO", Westinghouse Advanced Reactors Division, WARD-D-0005, (Rev. 4), (January 1976).
3. A. K. Agrawal, et al., "An Advanced Thermohydraulic Simulation Code for Transients in LMFBRs (SSC-L Code)", Brookhaven National Laboratory, BNL-NUREG-50773 (February 1978).
4. B. Donsky, "Complete Pump Characteristics and the Effects of Specific Speeds on Hydraulic Transients," ASME Transactions, Journal of Basic Engineering, pp. 685-696 (December 1967).
5. V. L. Streeter and E. B. Wylie, Hydraulic Transients, McGraw-Hill, New York (1967).
6. A. J. Stepanoff, "Centrifugal and Axial Flow Pumps: Theory, Design and Application," 2nd Edition, John Wiley & Sons, Inc. New York (1957).
7. P. W. Runstadler, Jr., "Review and Analysis of State-of-the-Art of Multiphase Pump Technology," Electric Power Research Institute, EPRI-159 (February 1976).
8. F. James and M. Roos, "MINUTS - "A package of programs to minimize a function of at most 15 variables, compute the covariance matrix and find the true errors," CERN Computer Center Program Library-D506.
9. R. Buonamici, "Summary Report of FFTF Prototype Primary Pump Sodium Test Program," Hanford Engineering Development Laboratory, HEDL-TME-77-106 (October 1977).

10. J.W. Yang and I.K. Madni, "Comparison of Pump Characteristics", in Reactor Safety Research Program, Quarterly Progress Report (July 1 - September 30, 1978), BNL-NUREG-50931, Brookhaven National Laboratory (1978).

11. Clinch River Breeder Reactor Project, Preliminary Safety Analysis Report, Project Management Corporation, (July 1975).

12. R.T. Knapp, "Complete Characteristics of Centrifugal Pumps and their use in the Prediction of Transient Behavior", ASME Transactions, Vol. 59, pp. 683-689 (1937).

13. D.J. Olson, "Single- and Two-Phase Performance Characteristics of the MOD-1 Semiscale Pump Under Steady State and Transient Fluid Conditions," Aerojet Nuclear Company, ANCR-1165, VC-78d (October 1974).

14. A. Batenburg, Westinghouse Advanced Reactors Division, private communication, (March 1978).

FIGURE CAPTIONS

1. Pump Configurations under Different Regimes of Operation.

2. Primary System Configuration for Two-Loop Simulation.

3. Comparisons with Experimental Data and IANUS Predictions for the FFTF Pump Performance.

4. Predicted and Measured Pump Head for the FFTF Pump.

5. Primary Pump Speed and Flow Decay for a Coastdown to Natural Circulation Transient in CRBR.

6. Transient Operating Points on Homologous Head Curves Following a Pipe Rupture Accident with $A_b = A_p$. a) Broken Loop Pump. b) Intact Loop Pump.

A.1 Flow Diagram to Determine Operating Regime, Curve Number, Head and Torque in Multi-Region Pump Characteristics.

TABLE CAPTIONS

1. Homologous Head and Torque Polynomial Coefficients (H,B≡Head or torque curve; A or V≡division by α^2 or ν^2; N,D,T or R≡normal, energy dissipation, turbine, or reverse pump region).

$\nu = Q/Q_R$

$\alpha = \Omega/\Omega_R$

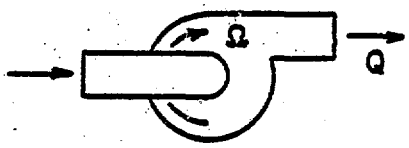

NORMAL PUMP
$(+\nu, +\alpha)$

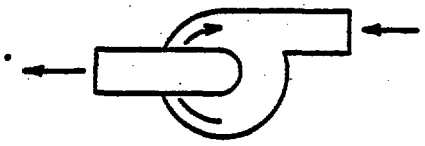

ENERGY DISSIP.
$(-\nu, +\alpha)$

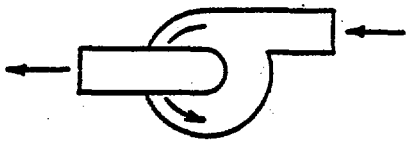

NORMAL TURBINE
$(-\nu, -\alpha)$

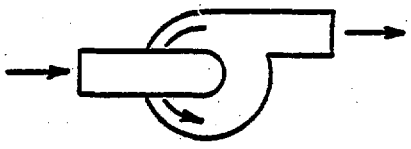

REVERSE PUMP
$(+\nu, -\alpha)$

Figure 1
Madni, I.K.

Table 1. Homologous head and torque polynomial coefficients (H,B≡head or torque curve; A or V≡division by α^2 or ν^2; N,D,T or R≡normal, energy dissipation, turbine, or reverse pump region)

Coeff. / (I) Curves	c_0	c_1	c_2	c_3	c_4	c_5
1 HVN	−0.556	0.85376	0.82906	−3.7106	7.0593	−3.4776
2 HAN+HAD	1.2897	−0.061907	0.17327	−0.57294	0.033762	0.13865
3 HVD	0.69189	0.43961	0.68459	−0.24701	0.63156	−0.20833
4 HVT	0.69209	−0.46132	0.92592	−0.4308	0.50845	−0.22436
5 HAT	0.63405	0.20178	−0.30242	0.76603	−0.48077	0.19231
6 HAR	0.63405	0.14665	−4.1896	−2.4828	6.99730	0.0
7 HVR	−0.556	0.66362	−0.086081	−0.93928	−0.57381	0.0
1 BVN	−0.37069	0.41741	3.8511	−7.6752	7.0695	−2.2917
2 BAN+BAD	0.44652	0.5065	0.59643	−0.64055	−0.025531	0.11531
3 BVD	0.8658	0.28437	−0.22348	0.45083	−0.70586	0.21562
4 BVT	0.86533	−0.60816	3.1497	−9.3647	10.418	−4.0064
5 BAT	−0.68468	1.8495	0.96871	−8.9653	12.045	−4.7546
6 BAR	−0.684	2.0342	−0.95477	−0.42286	0.0	0.0
7 BVR	−0.372	2.3716	−0.56147	0.0	0.0	0.0

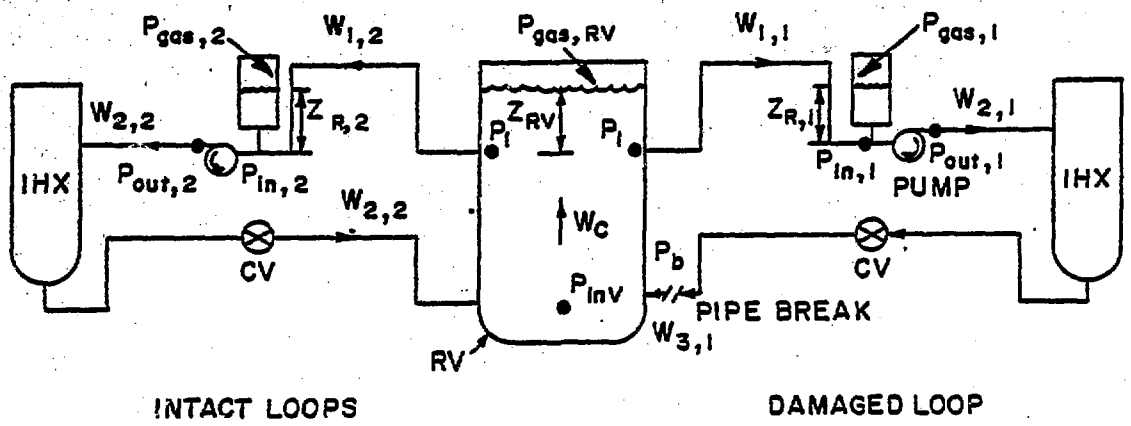

Figure 2
Madni, I.K.

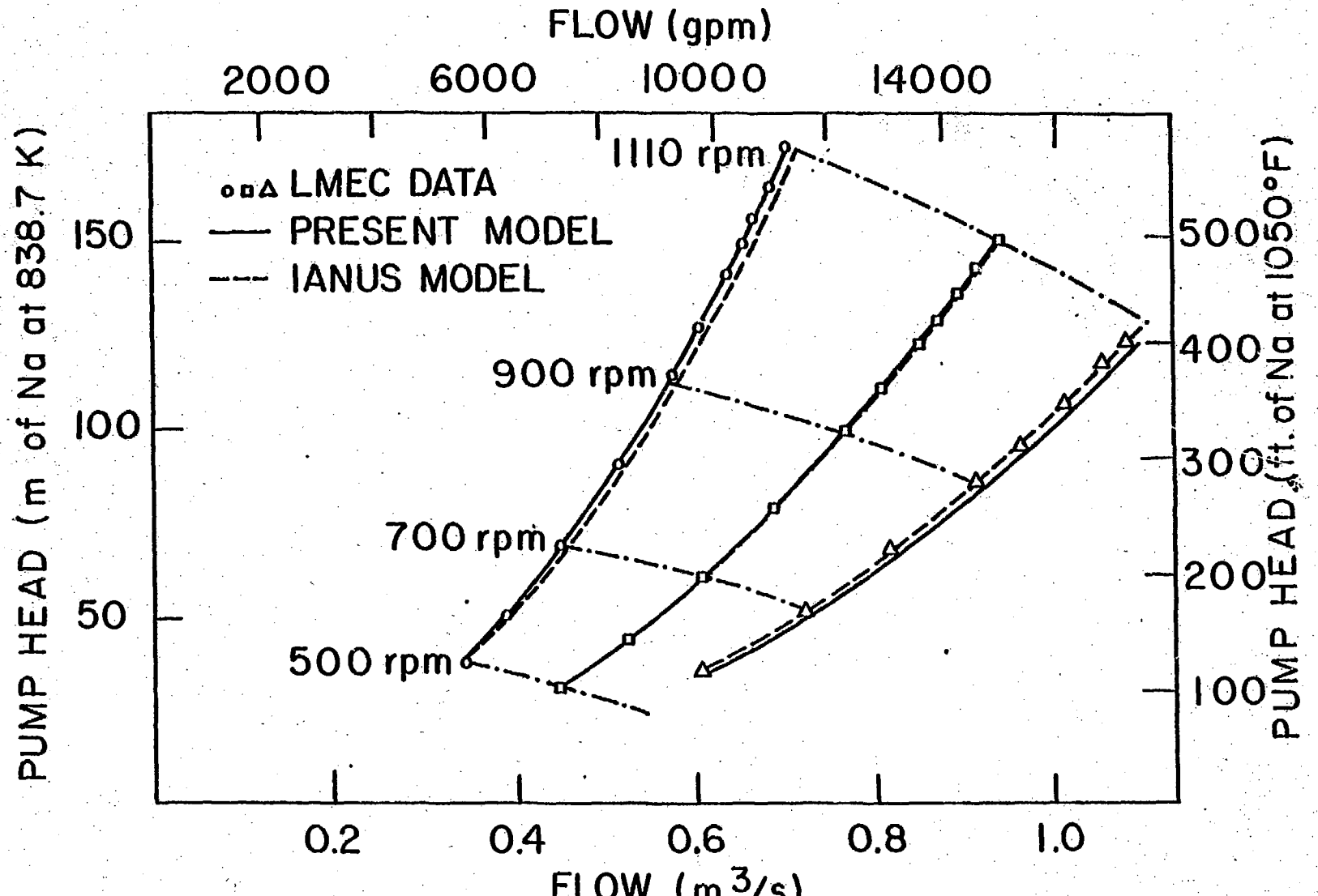
FLOW (gpm)
2000
6000
10000
14000
LMEC DATA
PRESENT MODEL
IANUS MODEL
1110 rpm
900 rpm
700 rpm
500 rpm
PUMP HEAD (m of Na at 838.7 K)
150
100
50
PUMP HEAD (ft. of Na at 1050°F)
500
400
300
200
100
0.2
0.4
0.6
0.8
1.0
FLOW (m3/s)

Figure 3

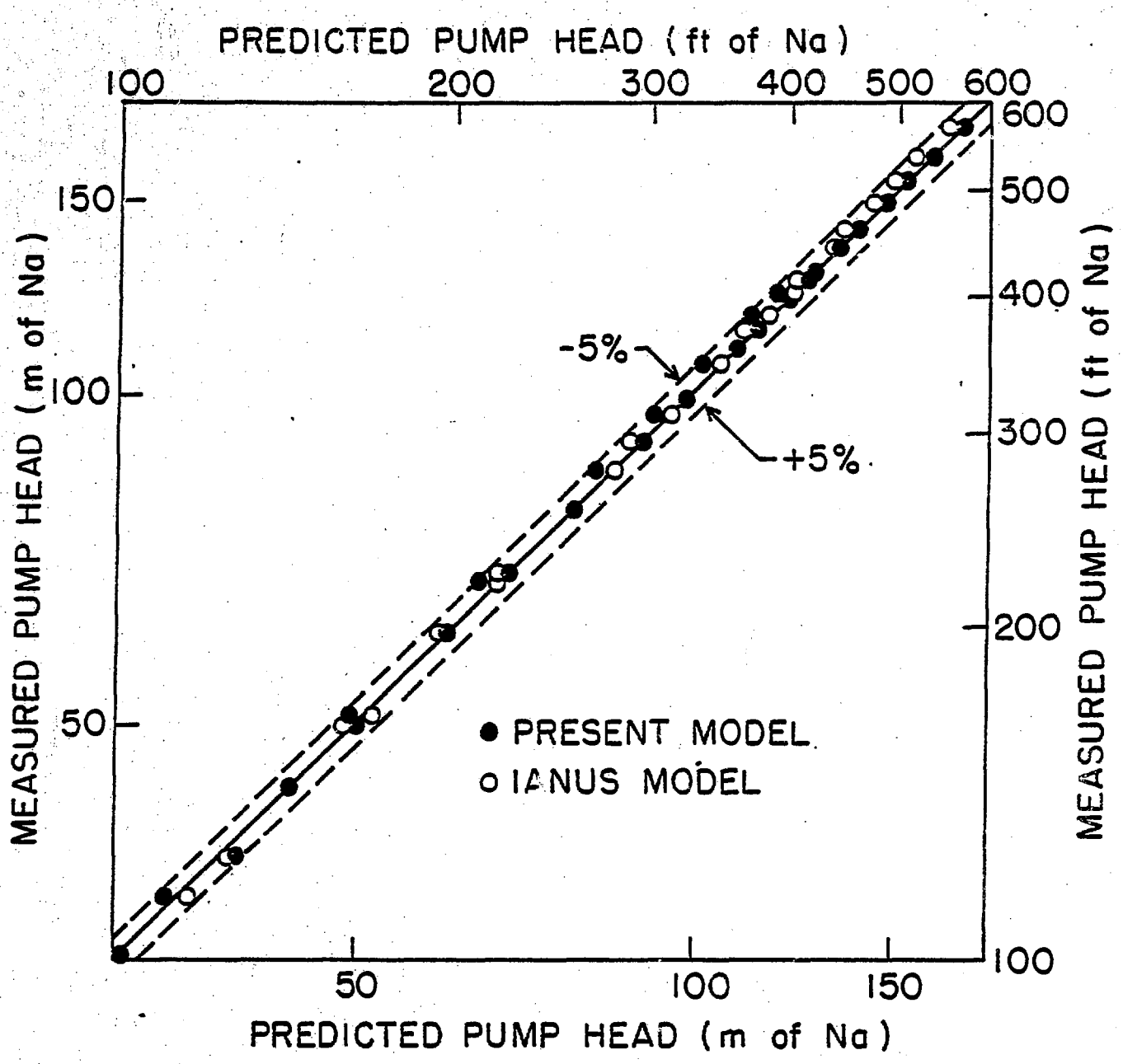

Figure 4
Madni, I.K.

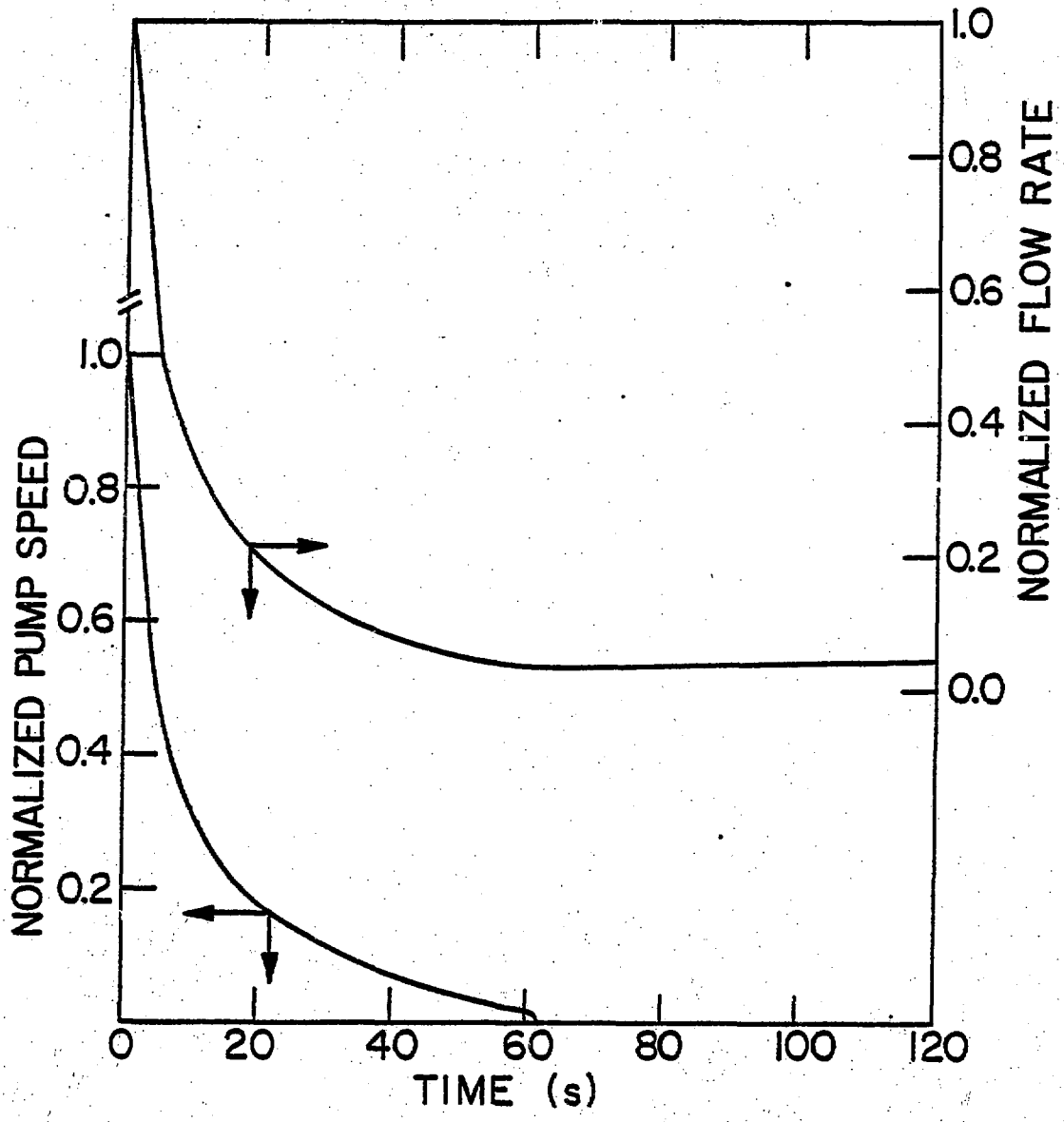

Figure 5
Madni, I.K.

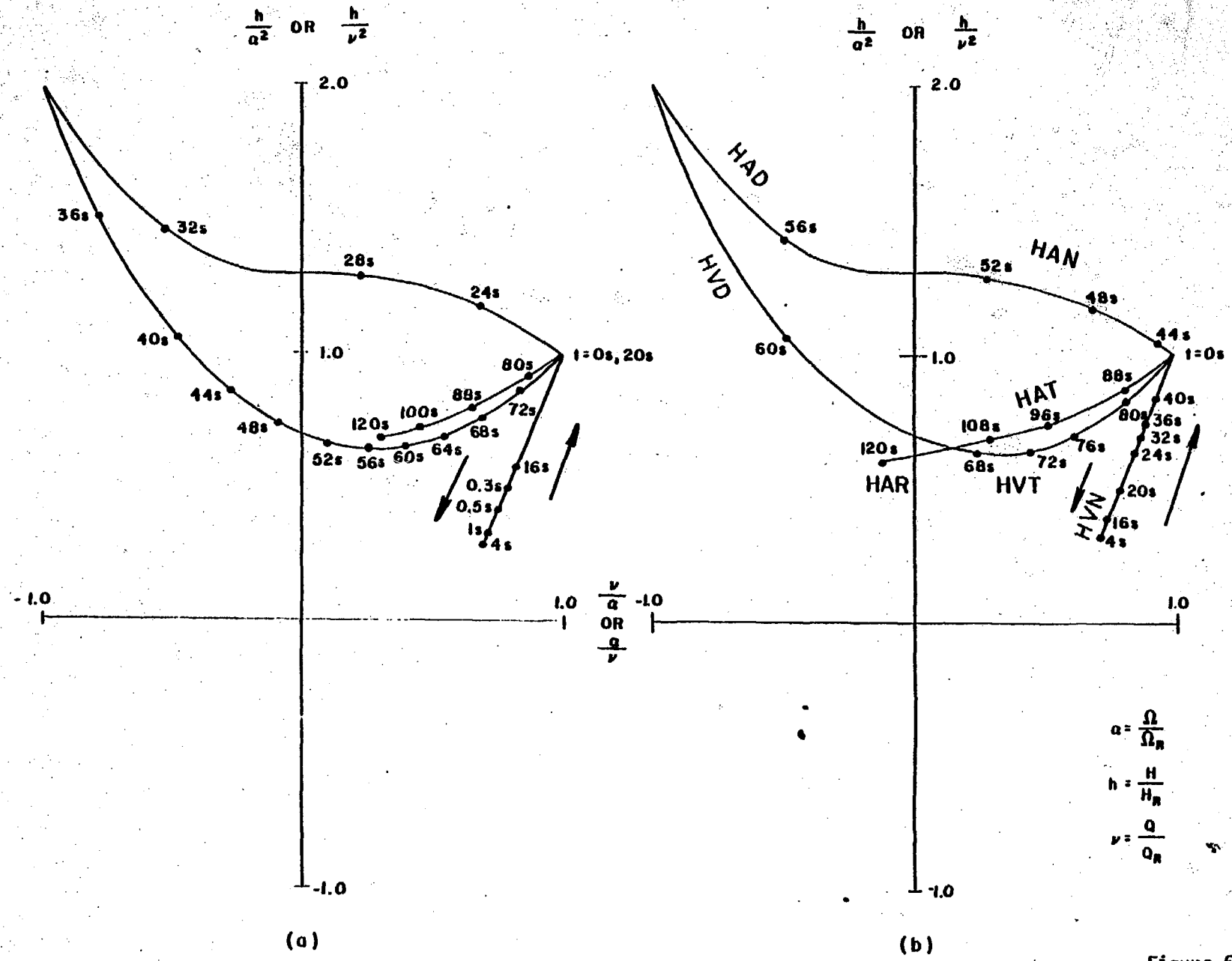

Figure 6
Madni, I.K.

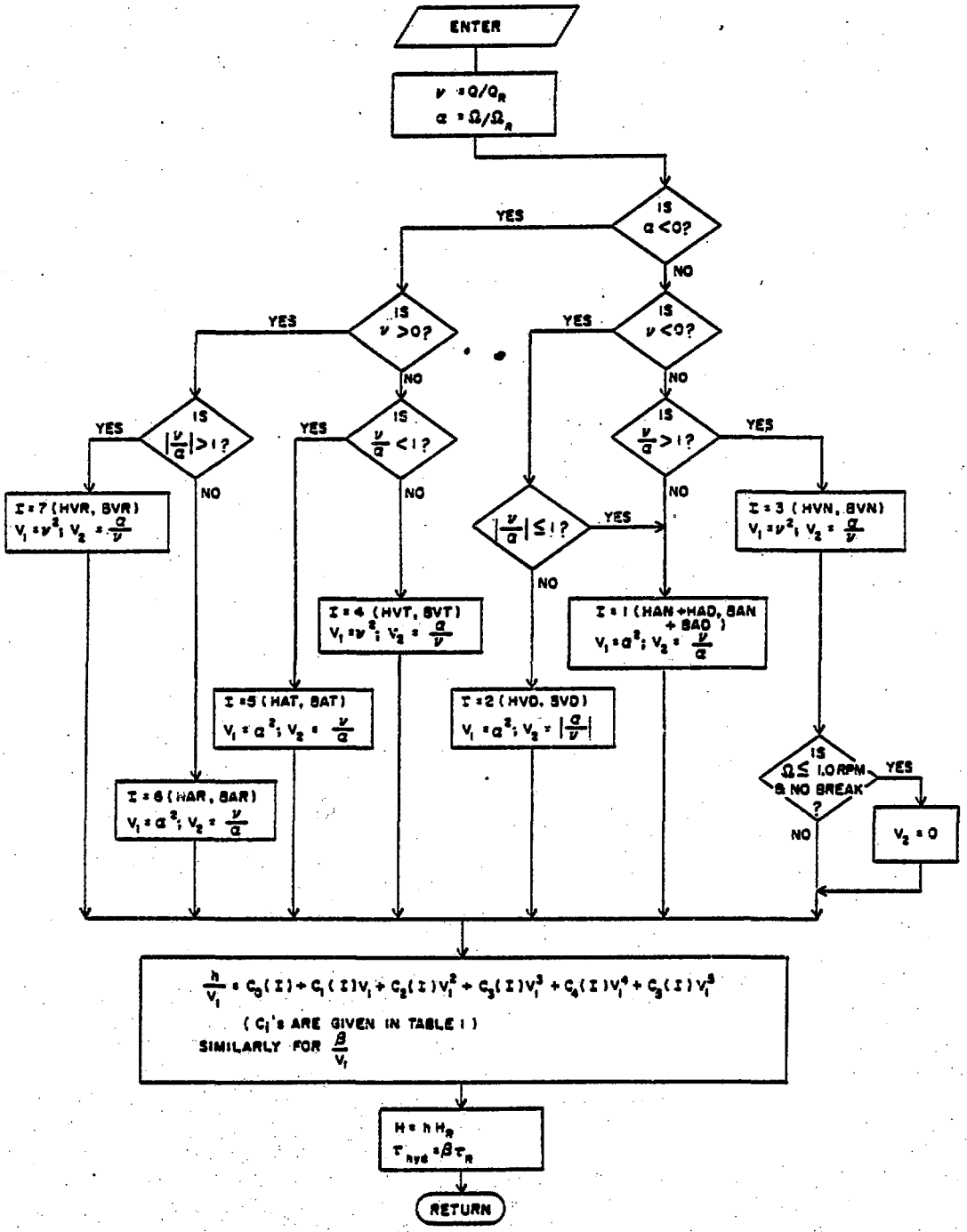

Figure A.1 FLOW DIAGRAM TO DETERMINE OPERATING REGIME, CURVE NUMBER, HEAD AND TORQUE IN MULTI-REGION PUMP CHARACTERISTICS